# Optimally Discretized Finite Elements for Boundary-Layer Stresses in Composite Laminates

S. S. Wang* and R. J. Stango†
*University of Illinois, Urbana, Illinois*

**A study of boundary-layer stresses in finite-width composite laminates is presented. Quasi three-dimensional, eight-node isoparametric elements are used in conjunction with a recently developed mesh optimization procedure. A consistent stress evaluation scheme is introduced to facilitate an accurate stress determination in a severely distorted mesh. Stresses near the laminate edge are obtained by the use of optimally discretized finite elements. For illustration, results from an optimized mesh consisting of 12 elements are shown to demonstrate the accuracy and efficiency of the current approach. Excellent agreement between the present solution and the singular laminate elasticity solution is obtained. Comparison with other finite element analyses having highly refined, nonoptimized grids is also reported to illustrate the superior performance of the present method.**

## I. Introduction

NEW and accelerated demands to employ structural composites in engineering applications have encouraged researchers to examine many aspects of the mechanics of composite materials. Of particular interest has been the complex behavior of stresses and related failure problems near the edge of composite laminates. The solution of such a problem requires the analysis of a layered, anisotropic material system with geometric boundaries. Due to the complex nature of the problem, various numerical studies have been attempted to determine the stresses and deformation in composites.[1-10] Upon examining a finite-width laminate subjected to uniform axial extension, early researchers noted that large stress gradients were evident as the laminate edge was approached. Thus a singularity had been postulated and, subsequently, various methods were employed in an effort to obtain an improved approximation of the stresses within the "boundary-layer" region of the laminate. Recently, the order of the edge-stress singularity for the laminate elasticity problem has been determined by an eigenfunction expansion method,[11] and associated edge stresses have been obtained by a boundary-collocation technique.[12]

Because of its versatility and simplicity, the finite element method has played a significant role in studying elasticity problem with singularities. It has been noted[13-15] that significantly improved solution accuracy and convergence can be achieved for this class of problems by the use of a singular element formulation or mesh optimization procedure. The singular finite element approach requires knowledge of the exact structure of the singular elasticity solution, and, therefore, the formulation is rather sophisticated.[15] The recently developed mesh optimization procedure in finite element analyses provides an attractive alternative for examining the singular elasticity problem. This approach has the advantage of using simple, conventional, nonsingular elements with much fewer degrees of freedom and, thus, solves the problem effectively and efficiently, as demonstrated in Refs. 13, 16, and 17. In this paper, a study of the boundary-layer stresses in composite laminates is presented by employing a suitable mesh optimization scheme in conjunction with a quasi three-dimensional finite element analysis.

In the next section, formulation of the quasi three-dimensional, eight-node isoparametric element is presented. The basic theory and procedure of mesh optimization for the problem are given in Sec. III. Discussion of a consistent stress-evaluation scheme for determining stresses along the ply interface in a composite laminate is reported in Sec. IV. Numerical examples are shown in Sec. V. Comparisons with the laminate elasticity solution and previous numerical analyses employing highly refined grids are made to illustrate the accuracy and efficiency of the present approach.

## II. Finite Element Formulation

In general, the complex stress state in a finite dimensional composite laminate warrants the use of three-dimensional elements. However, significant simplifications can be made by considering the well-known Pipes-Pagano problem,[2] which consists of a symmetric composite laminate under uniform axial extension, $\epsilon_z = \epsilon_0$ (Fig. 1). In this problem, the displacements $\boldsymbol{u}$ in the composite can be written as

$$\boldsymbol{u} = \boldsymbol{u}_0 + \boldsymbol{U}(x,y) \tag{1}$$

where

$$\boldsymbol{u}^T = \{u, v, w\} \tag{2a}$$

$$\boldsymbol{u}_0^T = \{0, 0, \epsilon_0 z\} \tag{2b}$$

$$\boldsymbol{U}^T = \{U(x,y), V(x,y), W(x,y)\} \tag{2c}$$

in which $U(x,y)$, $V(x,y)$, and $W(x,y)$ are unknown functions to be determined.

Using an isoparametric element representation for $U$, $V$, and $W$, one has

$$\boldsymbol{U} = \boldsymbol{N}\boldsymbol{q} \tag{3}$$

where $\boldsymbol{q}$ are nodal displacements (Fig. 2), and $\boldsymbol{N}$ is a matrix of nodal interpolation functions. The strain-displacement relationship has the form

$$\boldsymbol{\epsilon} = \boldsymbol{\epsilon}_0 + \boldsymbol{B}\boldsymbol{q} \tag{4}$$

where $\boldsymbol{\epsilon}^T = \{\epsilon_x, \epsilon_y, \epsilon_z, \gamma_{yz}, \gamma_{xz}, \gamma_{xy}\}$; $\boldsymbol{\epsilon}_0^T = \{0,0,\epsilon_0,0,0,0\}$; and $\boldsymbol{B}$ is the differentiated form of $\boldsymbol{N}(x,y)$. Because $\boldsymbol{N}$ is a function of $x$ and $y$ only, it is convenient to write Eq. (4) in the simplified form

$$\bar{\boldsymbol{\epsilon}}_{5\times 1} = \bar{\boldsymbol{B}}_{5\times 24}\boldsymbol{q}_{24\times 1} \tag{5}$$

Submitted Dec. 3, 1981; presented as Paper 82-0718 at the 23rd AIAA/ASME/ASCE/AHS Structures, Structural Dynamics and Materials Conference, New Orleans, La., May 10-12, 1982; revision received June 29, 1982. 

*Associate Professor, Department of Theoretical and Applied Mechanics. Member AIAA.

†Graduate Assistant, Department of Theoretical and Applied Mechanics.

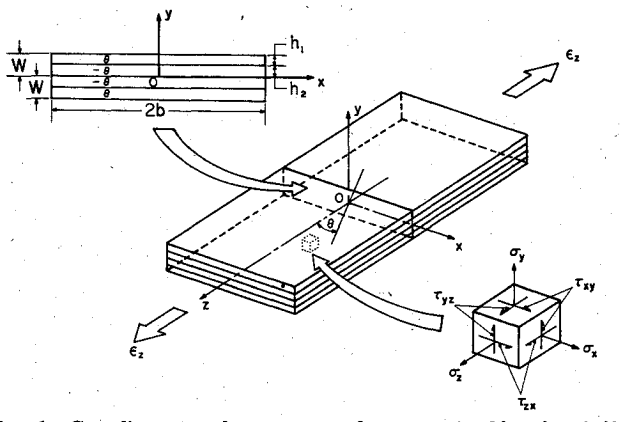


**Fig. 1 Coordinates and geometry of symmetric $[\theta/-\theta/-\theta/\theta]$ composite laminate subjected to uniform axial extension $\epsilon_z = \epsilon_0$.**

where $\bar{\epsilon}^T = \{\epsilon_x, \epsilon_y, \gamma_{yz}, \gamma_{xz}, \gamma_{xy}\}$, and $\bar{B}$ is the reduced form of the aforementioned gradient matrix, $B$.

The stress-strain relationship for a lamina in the composite under uniform axial strain, $\epsilon_0$, can be written in modified contracted notation[11]:

$$\bar{\sigma} = \bar{C}(\bar{\epsilon} - \bar{\epsilon}_0) \tag{6}$$

where

$$\bar{\sigma}^T = \{\sigma_x, \sigma_y, \tau_{yz}, \tau_{xz}, \tau_{xy}\} \tag{7a}$$

$$\bar{\epsilon}_0^T = \{\epsilon_{0i}\} = \{\epsilon_{0x}, \epsilon_{0y}, \gamma_{0yz}, \gamma_{0xz}, \gamma_{0xy}\} \text{ with } \epsilon_{0i} = (S_{i3}/S_{33})\epsilon_0 \tag{7b}$$

$$\bar{C}_{5\times5} = \bar{S}_{5\times5}^{-1} = \{\bar{S}_{ij}\}_{5\times5}^{-1} \qquad i,j = 1,2,4,5,6 \tag{8}$$

and $\bar{S}_{ij}$ is the reduced compliance tensor for each lamina.[11] The third stress component, $\sigma_z = \sigma_3$, is obtainable from

$$\sigma_3 = (\epsilon_0 - S_{3i}\sigma_i)/S_{33} \qquad i = 1,2,4,5,6 \tag{9}$$

From Eq. (6), it can be readily seen that $\bar{\epsilon}_0$ has the role analogous to that of initial strain.[18,19] Thus, in terms of $\bar{\epsilon}$ and $\bar{\epsilon}_0$, the potential energy functional, $\pi_p$, for an element can be written as follows:

$$\pi_p = \frac{1}{2}\iint_{A_m} \bar{\epsilon}^T \bar{C}\bar{\epsilon}\,dA - \iint_{A_m} \bar{\epsilon}^T \bar{C}\bar{\epsilon}_0\,dA + \frac{1}{2}\iint_{A_m} \bar{\epsilon}_0^T \bar{C}\bar{\epsilon}_0\,dA - \int_{S_{\sigma_m}} T^{*T} u\,ds + C_0 \tag{10}$$

where $T^*$ is the prescribed traction along the boundary $s_{\sigma m}$ of the $m$th element having area $A_m$, and $C_0$ is a constant related to $\epsilon_0$.

Following the standard procedure of the variational principle of minimum potential energy,[18,19] one can immediately obtain the element stiffness matrix $k$ and the consistent loading vector $Q$ as

$$k = \iint_{A_m} \bar{B}^T \bar{C}\bar{B}\,dA, \quad Q = \iint_{A_m} (N^T T^* + \bar{B}^T \bar{C}\bar{\epsilon}_0)\,dA \tag{11}$$

In the current study, the eight-node, quasi three-dimensional isoparametric element shown in Fig. 2 is used in the computation.

Equilibrium equations for the entire system can subsequently be written in a standard form by proper assemblage of element stiffness matrices. Nodal displacements and stresses at Gaussian stations inside an element are evaluated in the conventional manner.[18] A special interpolation/extrapolation scheme to be discussed in Sec. IV is employed for stress evaluation at laminate ply interfaces.

## III. Finite Element Mesh Optimization

In Sec. II, the potential energy $\pi_p$ is regarded as a function solely of the nodal displacements $q$. Accordingly, the potential energy must be minimized with respect to $q$ only, thereby resulting in one set of equilibrium equations. However, when the variational functional includes the mesh configuration, i.e., the nodal coordinates $x$, as an additional set of independent variables in the formulation, improved accuracy and rate of convergence can be achieved in the finite element solution.[13,20,21] Generally, in finite element mesh optimization the potential energy functional can be expressed as a function of both $q$ and $x$ as

$$\Pi = \sum_{m=1}^{n} \pi_p^{(m)}(q,x) \tag{12}$$

where $n$ is the total number of elements used in the discretization. The problem now becomes one of minimizing $\Pi$ with respect to both $q$ and $x$. Thus, on an element basis, one has[20-22]

$$\delta\pi_p = \frac{\partial \pi_p}{\partial q_i}\delta q_i + \frac{\partial \pi_p}{\partial x_j}\delta x_j = 0 \tag{13}$$

whereby the superscript $m$ is dropped for convenience. Hence the following equations can be readily established:

$$\frac{\partial \pi_p}{\partial q_i} = 0 \quad (i = 1,2,\ldots,3N), \qquad \frac{\partial \pi_p}{\partial x_j} = 0 \quad (j = 1,2,\ldots,2N) \tag{14}$$

where $N$ is the number of nodes ($N=8$) associated with the quasi-three-dimensional, eight-node isoparametric element used in the current study. These steps yield the following system of equations, respectively:

$$kq - Q = 0 \tag{15}$$

$$\frac{1}{2}q^T\frac{\partial k}{\partial x_j}q - q^T\frac{\partial Q}{\partial x_j} = 0 \qquad j = 1,2,\ldots,2N \tag{16}$$

For an arbitrary mesh, Eq. (16) is known to result in non-zero residuals[16,20] for *each* node associated with a given *element*. The *total* residuals associated with a node are computed by summing contributions of *all* elements having the common nodal coordinates $x_j$, as several elements can share the same node. Early investigators[20] constructed optimum grids based on minimization of the total residual terms. Recently, however, mesh optimization has been carried out by using a direct search procedure[21] based upon successive changes of nodal coordinates, leading to direct minimization of the total potential energy, $\Pi$, of the system:

$$\Pi(q,x) = \tfrac{1}{2}q^T K q - q^T Q + C^* \tag{17}$$

where $C^*$ is a constant due to the contribution of $\epsilon_0$. This method of obtaining an optimum mesh may be more convenient because the total potential energy of a system can be determined directly by summing contributions of all discrete elements, thereby circumventing the need for computing the aforementioned matrix gradients, $\partial k/\partial x_j$ and $\partial Q/\partial x_j$. Furthermore, this technique can be easily adapted to any finite element, regardless of the spatial dimension or the number of nodes associated with the element.

Due to the apparent advantages cited above, the method of direct minimization of total potential energy is employed for

the construction of optimal grids. To obtain the optimum mesh geometry, a search algorithm should be selected which repositions the nodal coordinates in the direction and location leading to rapid convergence. The particular algorithm suggested by Rosenbrock[23] is chosen to determine the optimum nodal locations in this investigation (see the Appendix). This method is adopted because of the previous successful results reported elsewhere[21] and the relative ease of implementation with a general purpose finite element program.[24]

## IV. Consistent Stress Evaluation Along Ply Interface

It is well known that, in a displacement-based finite element approach, stress and strain are commonly evaluated at selected integration points, i.e., Gaussian stations, within the element. In previous finite element analyses of the composite edge-stress problem, various averaging schemes have been proposed to evaluate stresses along the ply interface, and discrepancies among results have been reported.[9,10,25] Thus it is important that an accurate method be developed to compute stresses at certain desired locations within an element and along element boundaries, based upon stress values known elsewhere. This process involves interpolation and/or extrapolation of the results obtained from the finite element analysis. The method selected for this task must be consistent with the order of assumed interpolation functions and with the highly distorted element configuration in the optimally discretized mesh.

The variation of a particular stress component can be readily computed by appropriate differentiation of the assumed displacements in the natural coordinates, $\beta$ and $\eta$, of a severely distorted element with

$$u=U(\beta,\eta) \qquad v=V(\beta,\eta) \qquad w=\epsilon_0 z+W(\beta,\eta) \tag{18}$$

For example, from Eq. (1) the strain $\epsilon_x$ can be evaluated from

$$\epsilon_x=\frac{\partial u}{\partial x}=J^*_{11}u_{,\beta}+J^*_{12}u_{,\eta} \tag{19}$$

where $J^*_{ij}$ are associated with the inverted Jacobian[18] and the comma in the subscript of Eq. (19) denotes differentiation with respect to the subsequent variable. It is evident that for the eight-node isoparametric element used in this study the first term on the right side of the above expression is linear in $\beta$ and quadratic in $\eta$, whereas the second term is quadratic in $\beta$ and linear in $\eta$. Thus, appropriate numerical formulas should lead to a quadratic variation of the stress component $\sigma_x$ if interpolation/extrapolation is performed along $\eta$, where $\beta=$const (Fig. 3a). Variations of the remaining stress components along $\eta$ follow the same argument.

Essential features of the interpolation/extrapolation scheme used in the current study are illustrated in Figs. 3a and 3b. In Fig. 3a, for example, stresses $\sigma_i^{(k)}$ $(k=1,2,3)$ determined from the finite element solution at three different Gaussian stations along $\beta=$const are shown within an element located adjacent to the ply interface. The stress distribution along $\eta$ with $\beta=$const can be evaluated by employing Lagrange's interpolation formula[26]:

$$\sigma_i(\eta)=\frac{(\eta-\eta_2)(\eta-\eta_3)}{(\eta_1-\eta_2)(\eta_1-\eta_3)}\sigma_i^{(1)}+\frac{(\eta-\eta_1)(\eta-\eta_3)}{(\eta_2-\eta_1)(\eta_2-\eta_3)}\sigma_i^{(2)}$$
$$+\frac{(\eta-\eta_1)(\eta-\eta_2)}{(\eta_3-\eta_1)(\eta_3-\eta_2)}\sigma_i^{(3)} \qquad \eta_1\le\eta\le\eta_3 \tag{20}$$

Ply interface stress $\sigma_i^{(I)}$ can be obtained by extrapolation to the lamina interface (i.e., point $I$ with $\eta=\pm1$ in Figs. 3a and 3b) using the following equation[27]:

$$\sigma_i^{(I)}=\sigma_i^{(A)}+\left.\frac{d\sigma_i}{d\eta}\right|_A d+\frac{1}{2h}\left(\left.\frac{d\sigma_i}{d\eta}\right|_A-\left.\frac{d\sigma_i}{d\eta}\right|_B\right)d^2 \tag{21}$$

where, as depicted in Fig. 3b, A and B refer to the locations at which the stresses and stress gradients are evaluated along the $\beta=$constant line; $h$ is the interval chosen between A and B; and $d$ is the distance to the element edge from point A. Note that Eq. (21) does not utilize endpoints of the data, thereby avoiding difficulties in the numerical approximation. Generally, the use of Eq. (21) can yield a slight discrepancy between interlaminar stress, $\sigma_i^{(I)}$, computed at common boundary points of finite elements located above and below the lamina interface (i.e., at $y=h^+$ and $y=h^-$). In the current research, average values are reported for interlaminar stresses, $\sigma_i^{(I)}$ $(i=2,4,6)$, along the ply interface.

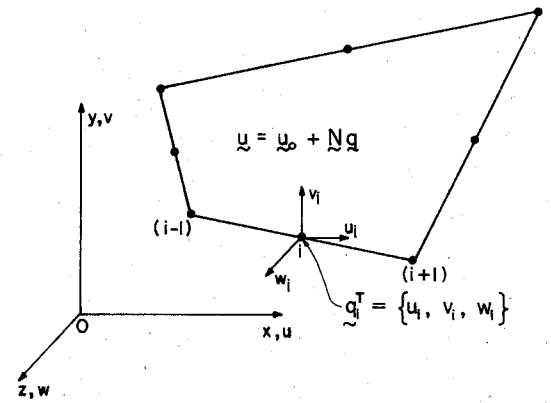


Fig. 2 Eight-node, quasi-three-dimensional isoparametric element.

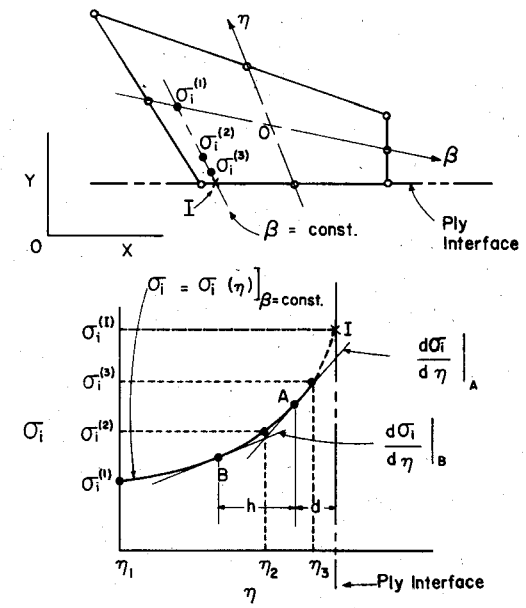


Fig. 3 Consistent stress-evaluation scheme along ply interface; a) stresses at Gaussian stations along $\beta=$const, and b) extrapolation scheme to ply interface.

## V. Results and Discussion

In this section a rationale for selecting an initial finite element mesh geometry from which an optimum grid is constructed will be presented first. Solutions obtained from the optimized mesh are compared with the analytical solution[12] and the results[9,15] from highly refined grids reported in the literature. Apparent advantages of the current approach are also discussed.

The geometric configuration and loading condition of the laminate elasticity problem analyzed appear in Fig. 1. Ply elastic constants used in the analysis are as follows‡:

$$E_{11}=E_{22}=14.48\text{ GPa }(2.1\times10^6\text{ psi})$$

$$E_{33}=137.9\text{ GPa }(20\times10^6\text{ psi})$$

$$G_{12}=G_{31}=G_{32}=5.86\text{ GPa }(0.85\times10^6\text{ psi})$$

$$\nu_{12}=\nu_{31}=\nu_{32}=0.21 \tag{22}$$

where subscripts *1*, *2*, and *3* refer to transverse, thickness, and fiber directions, respectively. Laminate dimensions and geometry for the $[\theta/-\theta/-\theta/\theta]$ graphite-epoxy composite are specified as follows: $h_1=h_2=2.54$ cm (1.0 in.), $b=20.32$ cm (8.0 in.), and $\theta=\pi/4$. Material and geometric symmetry conditions permit that only one-quarter of the laminate cross section be examined.

### A. Grid Optimization

In general, the aforementioned iterative technique employed to obtain an optimum grid requires significant computational effort. If the number of active degrees of freedom, i.e., the number of nodal coordinates to be repositioned, is not maintained to a sufficiently small quantity, the total effort involved can render optimization uneconomical. Therefore initial mesh selection is an important step in the overall procedure of grid optimization.

To reduce the computational effort in the current problem, the mesh of the upper ply in the laminate appearing in Fig. 4a is initially selected for optimization. Owing to the approximately symmetric nature of the stresses about the ply interfaces in the $[\theta/-\theta/-\theta/\theta]$ composite,[9,12] a nearly optimum mesh for the quarter-laminate cross section can be subsequently constructed. In Figs. 4a-d, the updated grid geometries and associated potential energy, $\Pi$, at several stages of the optimization process are reported. The variations of both mesh geometry and $\Pi$ associated with each stage are related to the minimization of potential energy functional and solution convergence, as discussed in the Appendix. The final mesh configuration and potential energy level appear in Fig. 5. The convergence criterion employed in the present optimization requires that changes of all nodal coordinates during iteration satisfy

$$\left|\frac{x^{(i+1)}-x^{(i)}}{x^{(i)}}\right|\le 0.01 \tag{23}$$

where $x^{(i)}$ are the coordinates of each active node in the $i$th iterative step.

In attempting to establish an optimum mesh geometry for an elasticity problem with stress singularity, one notes that the nodes in the vicinity of the singular point tend to gather arbitrarily close; thus abnormal effects upon solution stability and convergence usually occur. This situation can be remedied by the use of a constraining parameter, $\delta_s$, for the near-field element to prevent any node from approaching arbitrarily close to the singular point. Thus linear element dimensions adjacent to the singular point are required to exceed the prescribed $\delta_s$. In the current study, $\delta_s/h_1=0.15$ is employed. Selection of this numerical value is motivated by previous mesh optimization studies of singular elasticity problems.[17]

‡Values of the shear modulus $G_{12}$ and Poisson's ratio $\nu_{12}$ employed here, which were also used in previous studies,[2,9,12] are recognized to be hypothetical and are only for illustration of the general nature of the present problem. More appropriate values for the properties are $\nu_{12}\simeq1.5\,\nu_{31}=0.32$ and $G_{12}\simeq0.6\,G_{31}=3.52$ GPa ($0.51\times10^6$ psi). The results obtained by using these more appropriate elastic constants differ from those given in this paper by approximately 10%.[28]

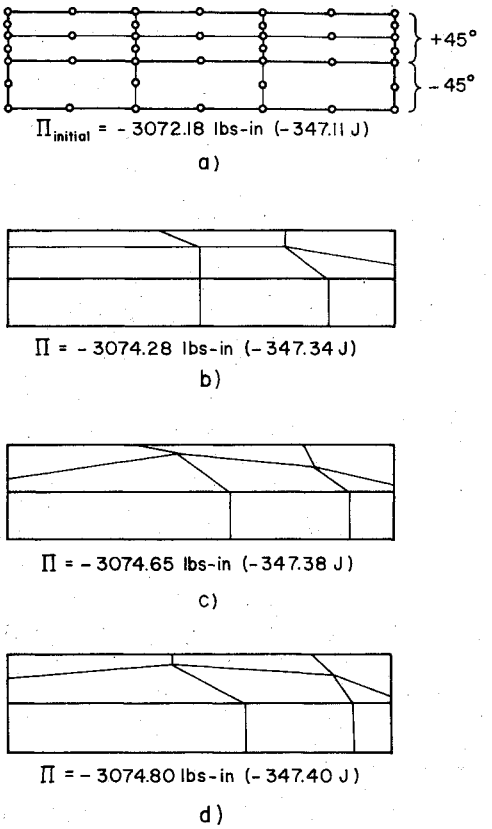


**Fig. 4 Mesh configurations and associated potential energy levels at various stages of minimization of Π.**

### B. Current Results and Comparison with Existing Solutions

In this study, solutions from the optimum mesh using eight-node isoparametric elements are obtained and compared with previous results reported elsewhere. For illustrative purposes, the solution from the 12-element ($N=12$) optimal mesh (Fig. 5) for the $[\pm45]_s$ composite laminate under uniaxial strain, $\epsilon_0$, is presented. The elasticity solution[11,12] obtained by an eigenfunction expansion method is given as a reference. Previous results derived from highly refined grids consisting of conventional constant-strain triangular (CST)[9] and eight-node isoparametric elements[15] are also included for comparison. In general, the optimum-mesh finite element solution for in-plane and interlaminar stresses is observed to be consistently more accurate than that given by the nonoptimum, highly refined grids.

For example, the in-plane normal and shear stresses, $\sigma_x$, $\sigma_z$, and $\tau_{xz}$, along the 45- and $-45$-deg ply interface are shown by open circles in Fig. 6. Solutions derived from locally enriched CST elements and eight-node isoparametric elements are also given.[9,15] With very few elements (e.g., $N=12$), the current solution is in excellent agreement with the reference singular elasticity solution.[12] Even with ten times more elements (Fig. 6), conventional mesh arrangements provide results[9,15] with significant discrepancies in the vicinity of the laminate edge.

A significant difference is also observed for the interlaminar shear component $\tau_{xy}$ shown in Fig. 7a. The solution from the optimized mesh is in close agreement with the elasticity solution,[12] whereas the results of earlier research[9] exhibit a readily apparent discrepancy. Results for the most dominant interlaminar shear stress, $\tau_{yz}$, shown in Fig. 7b, however, are consistent with those obtained by using different approaches.

The interlaminar normal stress, $\sigma_y$, along the ply interface obtained by various approaches is shown in Fig. 8. A compressive $\sigma_y$ is observed from the present optimum mesh solution, whereas a tensile interlaminar normal stress is given

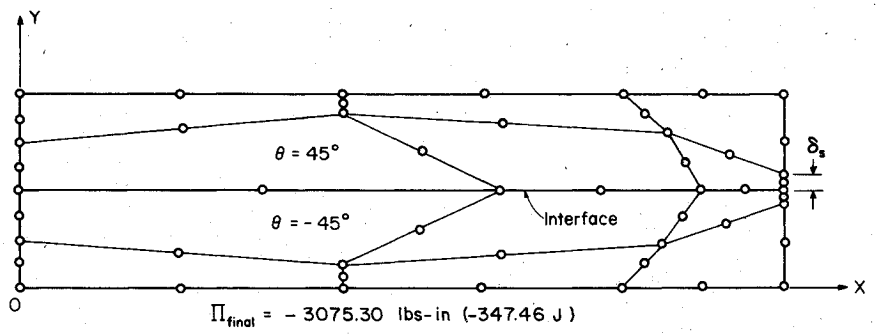


Fig. 5 Optimal finite element mesh for boundary-layer stress calculation.

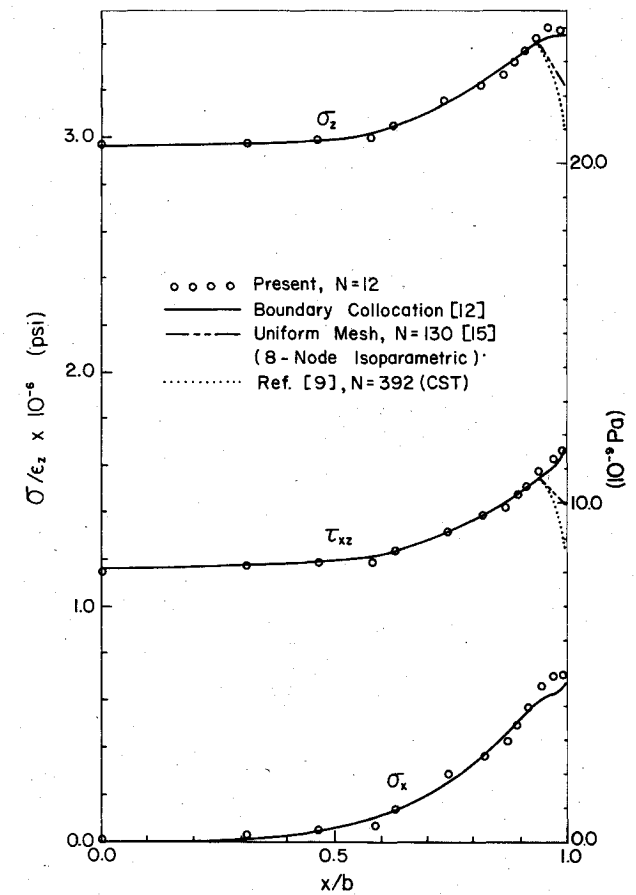


Fig. 6 Comparison of present solution for $\sigma_x$, $\sigma_z$, and $\tau_{xz}$ along ply interface $y=h$ with reference solutions for [45/−45/−45/45] graphite-epoxy composite.

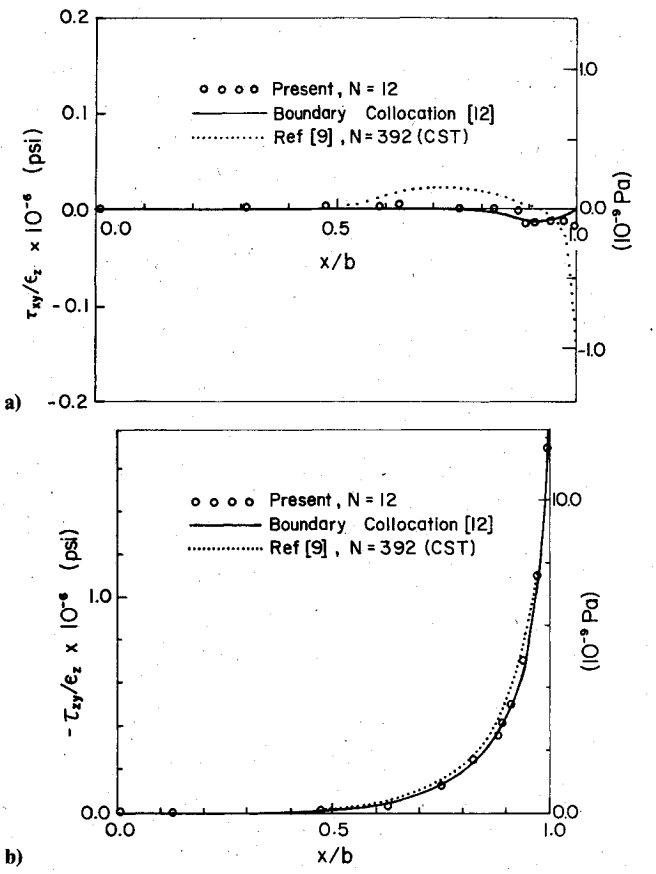


Fig. 7 a) Comparison of present solution for $\tau_{xy}$ along ply interface $y=h$, with reference solutions for [45/−45/−45/45] graphite-epoxy composite. b) Comparison of present solution for $\tau_{yz}$ along ply interface $y=h$ with reference solutions for [45/−45/−45/45] graphite-epoxy composite.

by Ref. 9. The correctness of the present solution (sign and magnitude) is confirmed by an independent elasticity solution[12] and by a recently developed singular hybrid finite element analysis.[15] It is observed (Fig. 8) that the present results for $\sigma_y$ are in remarkable agreement with the singular elasticity solution.[12]

In Fig. 9, through-thickness performance of the optimum mesh for the shear stress $\tau_{yz}$ is clearly demonstrated. Examining the reference solution[12] at the laminate edge ($x/b=1.0$), one observes that this shear component increases very rapidly from the laminate surface and midplane ($y/h=2.0$ and 0.0), where $\tau_{yz}=0$, to the ply interface ($y/h=1.0$), where the shear stress becomes unbounded. The present solution employs only two elements per ply through the laminate-thickness direction. The nature of the current finite element formulation permits $\tau_{yz}$ to vary, at best, linearly in the thickness direction within each element. However, excellent agreement with the elasticity solution[12] is obtained for the through-thickness distribution of $\tau_{yz}$. This result can be attributed to both the mesh optimization and the aforementioned consistent stress-evaluation scheme.

### C. Additional Remarks

It has been a common practice in previous finite element and finite difference analyses of singular laminate elasticity problems to use various arbitrary local grid enrichment in an attempt to obtain an acceptable near-field solution. Such a trial-and-error procedure has been shown to result in very large computational effort, time-consuming data planning and preparation, and an elaborate stress averaging technique, which might, nevertheless, yield controversial results. Thus the need for obtaining a more accurate solution to the present problem, while maintaining numerical simplicity as in the current approach, is apparent. However, the approximate nature of the current finite element approach can not provide an analytical structure of the singular laminate elasticity

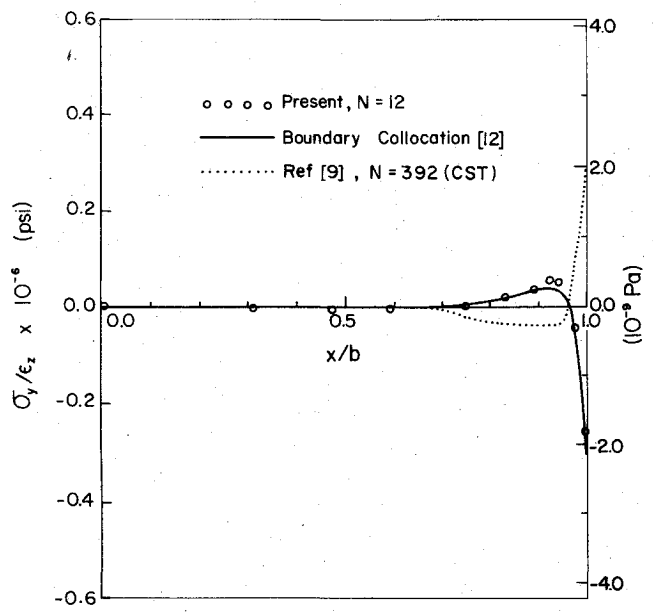


**Fig. 8 Comparison of present solution for $\sigma_y$ along ply interface $y=h$ with reference solutions for [45/−45/−45/45] graphite-epoxy composite.**

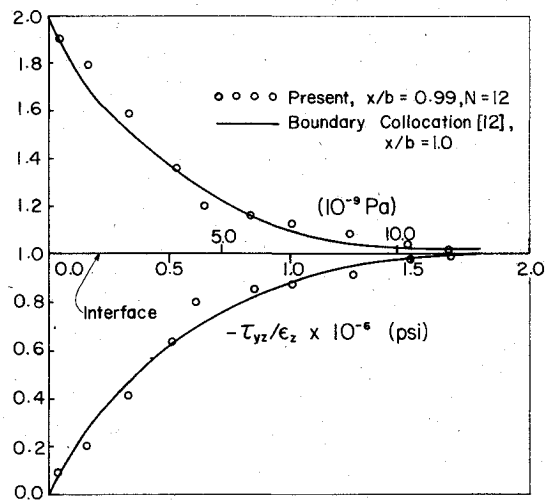


**Fig. 9 Comparison of present solution for $\tau_{yz}$ through laminate thickness at $x/b \simeq 1.0$, with reference solution for [45/−45/−45/45] graphite-epoxy composite.**

solution, i.e., the strength (or the order) of the boundary-layer stress singularity.

Using a more sophisticated hybrid finite element formulation,[15] one can include the exact singular structure of the elasticity solution for the current problem. The efficiency of the present numerical approach relative to the hybrid finite element method is also of interest in this study. A comparison of the numerical algorithms for the two approaches to the boundary-layer problem having the same degree of discretization (i.e., with 12 elements and 51 nodes) indicates that slightly less CPU time for the optimal mesh ($t_0 = 120$ s) is needed than that of the hybrid finite element approach ($t_h = 135$ s).

## VI. Summary and Conclusions

The present research has demonstrated that excellent results can be achieved when the following considerations are properly included in analyzing the composite boundary-layer stress problem: 1) suitable element selection, 2) optimum mesh discretization, and 3) compatible method for stress evaluation. An accurate solution for laminate edge stresses is provided along with significantly reduced computational effort and expense for this class of problems.

Based on the aforementioned method of analysis and numerical results in this paper, the following conclusions can be reached:

1) The current approach yields numerical solutions which are in excellent agreement with the existing singular laminate elasticity solution.

2) The mesh optimization and the consistent stress-evaluation scheme provide solutions with greater accuracy than those from a conventional finite element analysis with an arbitrarily enriched mesh.

3) The present numerical approach is demonstrated to be very efficient and effective in dealing with laminate elasticity problems having a stress singularity.

It is further noted that the current computational methodology and strategy can be extended to problems of similar nature, e.g., other singular elastic, thermoelastic and viscoelastic problems, which are discussed in related papers.[29,30]

## Appendix

Optimization of a finite element grid used in this study is based upon a minimization scheme stated in Sec. III. An algorithm for minimization of a functional, as proposed by Rosenbrock,[23] is briefly outlined here to illustrate the scheme used for successively reducing the total potential energy by appropriately repositioning the nodal coordinates.

Basically, the method employs an algorithm of recurrent coordinate transformation with a continuous search for an optimal path to minimize the objective functional. For example, by considering a function of two variables, $\Pi(x_1,x_2)$, the method can be illustrated schematically as follows:

1) An initial step of arbitrary length, $e$, and directional unit vector $\xi_1^0$ coincident with the coordinate axis $x_1$, as shown in

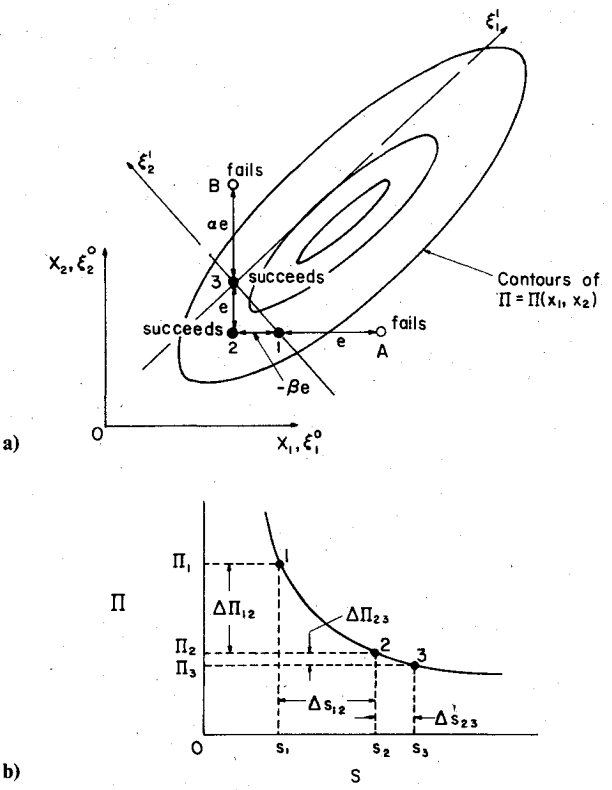


**Fig. A1 Algorithm for minimizing potential energy functional Π. a) Direct search for minimum Π by successive coordinate transformation; b) corresponding potential energy level for each successful trial.**

Fig. A1a is assumed for convenience. The superscripts designate the stage number, as will be defined later.

2) If a lower value of $\Pi$ results (termed as a "success") from the above trial, then $e$ is multiplied by $\alpha(>1)$. However, if the initial step does not succeed, then $e$ is multiplied by $-\beta(0<\beta<1)$. For example, $\Pi$ is sampled at an arbitrary point 1 (Figs. A1a and A1b). An initial step $e$ is taken along the $\xi_1^0$ direction, and fails at point A; subsequently, the step $-\beta e$ is taken and succeeds at point 2. Each step taken is termed as a "trial." Such trials continue until at least one success and one failure is encountered for each variable. Then, the next step taken is in the $\xi_2^0$ direction, and succeeds at point 3; subsequently, a step $\alpha e$ is taken to point B, where a failure is noted. When all variables have experienced at least one successful and unsuccessful trial, a "stage" is completed.

3) At the completion of each stage, an orthogonal set of new coordinates, $\xi_1^1$ and $\xi_2^1$, for further searching is constructed by a procedure described in Ref. 17.

The foregoing procedure continues until the convergence criterion discussed in Sec. V is satisfied. A generalization of the present method to "$n$" dimensions is discussed by Rosenbrock[23] in sufficient detail to facilitate its direct use.

## Acknowledgments

The research reported in this paper is supported in part by a U.S. Navy Grant N00014-79-C-0579 from the Office of Naval Research (ONR) to the University of Illinois. The authors wish to express their gratitude to Dr. N. Perrone and Dr. Y. Rajapakse of ONR for the support and encouragement, to Prof. R. E. Miller and F. G. Yuan of the Department of Theoretical and Applied Mechanics, University of Illinois, and Prof. L. L. Durocher, Department of Mechanical Engineering, University of Bridgeport, for fruitful discussion and suggestions. Appreciation is also extended to Mrs. Darlene Mathine for typing the manuscript. Computer time provided by the Research Board of the University of Illinois is gratefully acknowledged.

## References

[1] Puppo, A. H. and Evensen, H. A., "Interlaminar Shear in Laminated Composites Under Generalized Plane Stresses," *Journal of Composite Materials*, Vol. 4, April 1970, pp. 204-220.

[2] Pipes, R. B. and Pagano, N. J., "Interlaminar Stresses in Composite Laminates Under Uniform Axial Extension," *Journal of Composite Materials*, Vol. 4, Oct. 1970, pp. 538-548.

[3] Whitney, J. M., "Free-Edge Effects in the Characterization of Composite Materials," *Analysis of the Test Methods for High Modulus Fibers and Composites, ASTM STP 521*, American Society for Testing and Materials, 1973, pp. 167-180.

[4] Pipes, R. B., Kaminski, B. E., and Pagano, N. J., "Influence of the Free Edge Upon the Strength of Angle Ply Laminates," *Analysis of the Test Methods for High Modulus Fibers and Composites, ASTM STP 521*, American Society for Testing and Materials, 1973, pp. 218-228.

[5] Pagano, N. J., "On the Calculation of Interlaminar Normal Stress in Composite Laminates," *Journal of Composite Materials*, Vol. 8, Jan. 1974, pp. 65-81.

[6] Hsu, P. W. and Herakovich, C. T., "Edge Effects in Angle-Ply Composite Laminates," *Journal of Composite Materials*, Vol. 11, Oct. 1977, pp. 422-428.

[7] Tang, S. and Levy, A., "A Boundary Layer Theory—Part II: Extension of Laminated Finite Strip," *Journal of Composite Materials*, Vol. 9, Jan. 1975, pp. 42-45.

[8] Pagano, N. J., "Free-Edge Stress Fields in Composite Laminates," *International Journal of Solids and Structures*, Vol. 14, No. 5, 1978, pp. 401-406.

[9] Wang, A.S.D. and Crossman, F. W., "Some New Results on Edge Effects in Symmetric Composite Laminates," *Journal of Composite Materials*, Vol. 11, Jan. 1977, pp. 92-106.

[10] Spilker, R. L. and Chou, S. C., "Edge Effects in Symmetric Composite Laminates," *Journal of Composite Materials*, Vol. 14, Jan. 1980, pp. 2-20.

[11] Wang, S. S. and Choi, I., "Boundary-Layer Effects in Composite Laminates: Part I—Free-Edge Stress Singularities," *Journal of Applied Mechanics, Transactions of ASME*, Vol. 49, No. 3, Sept. 1982, pp. 541-548.

[12] Wang, S. S. and Choi, I., "Boundary-Layer Effects in Composite Laminates: Part II—Free-Edge Stress Solutions and Basic Characteristics," *Journal of Applied Mechanics, Transactions of ASME*, Vol. 49, No. 3, Sept. 1982, pp. 549-560.

[13] Shephard, M. S., Gallagher, R. H., and Abel, J. F., "Finite Element Solutions to Point-Load Problems," *Journal of Engineering Mechanics Division, Proceedings of American Society of Civil Engineers*, Vol. 107, No. EM5, Oct. 1981, pp. 839-850.

[14] Tong, P. and Pian, T.H.H., "On the Convergence of the Finite Element Method for Problems with Singularity," *International Journal of Solids and Structures*, Vol. 9, No. 3, 1973, pp. 313-321.

[15] Wang, S. S. and Yuan, F. G., "A Singular Hybrid Finite Element Analysis of Boundary-Layer Stresses in Composite Laminates," *International Journal of Solids and Structures*, (in press), 1983.

[16] Durocher, L. L. and Stango, R. J., "Finite Element Mesh Optimization and Enrichment Techniques," *Structural Mechanics Software Series*, Vol. 3, edited by N. Perrone, and W. Pilkey, University Press of Virginia, Charlottesville, Va., 1980, pp. 245-262.

[17] Stango, R. J., "Optimum Grid Selection for Finite Element Analyses," M.S. Thesis, Department of Mechanical Engineering, University of Bridgeport, Bridgeport, Conn., May 1977.

[18] Zienkiewicz, O. C., *The Finite Element Method*, 3rd ed., McGraw-Hill, London, 1977.

[19] Desai, C. S. and Abel, J. F., *Introduction to the Finite Element Method*, Van Nostrand Reinhold, New York, 1972.

[20] McNeice, G. M. and Marcal, P. V., "Optimization of Finite Element Grids Based on Minimum Potential Energy," *Journal of Engineering for Industry*, Vol. 95, No. 1, 1973, pp. 186-190.

[21] Turcke, D. J., "On Optimum Finite Element Grid Configurations," *AIAA Journal*, Vol. 14, No. 2, Feb. 1976, pp. 264-265.

[22] Carroll, W. E., "Inclusive Criteria for Optimum Grid Generation in the Discrete Analysis Technique," *Computers and Structures*, Vol. 6, Aug./Oct. 1976, pp. 333-337.

[23] Rosenbrock, H. H., "An Automatic Method for Finding the Greatest or Least Value of a Function," *The Computer Journal*, Vol. 3, Oct. 1960, pp. 175-184.

[24] *Fortran IV Subroutine "Climb,"* University of Waterloo Computing Center, 1971.

[25] Herakovich, C. T., Nagarkar, A., and O'Brien, D. A., "Failure Analysis of Composite Laminates with Free Edges," *Modern Developments in Composite Materials and Structures*, edited by J. R. Vinson, American Society of Mechanical Engineers, 1979, pp. 53-56.

[26] Scarborough, J. B., *Numerical Mathematical Analysis*, 6th ed., The John Hopkins Press, Baltimore, Md., 1966, p. 74.

[27] Ralston, A. and Rabinowitz, P., *A First Course in Numerical Analysis*, International Series of Pure and Applied Mathematics, McGraw-Hill, New York, 1978.

[28] Wang, S. S., Department of Theoretical and Applied Mechanics, University of Illinois, Urbana, Ill., unpublished research data, 1982.

[29] Stango, R. J. and Wang, S. S., "Process-Induced Residual Thermal Stresses in Advanced Fiber-Reinforced Composite Laminates," *Polymer Processing: Analysis and Innovation*, edited by N. Suh and C.L. Tucker, ASME-PED—Vol. 5, American Society of Mechanical Engineers, 1982, pp. 67-81.

[30] Wang, S. S., Stango, R. J., and Durocher, L. L., "A Finite Element Mesh Optimization Approach to Elasticity Problems with Stress Singularities," (in preparation), 1983.